Reactive Power Compensation using Fuzzy Gain Scheduling (FGS) based PID Controller of Synchronous Machine

Maamoon F. Al-Kababji **Ahmed N. B. Alsammak**
Email: Alkababji@yahoo.com **Email: Ahmed_Alsammak2003@yahoo.com**

Electrical Engineering Department - University of Mosul

Abstract

Application of Fuzzy Logic (FL) theory to self-tuning PID controller for the reactive power compensation using Synchronous Machine (SM) is investigated in this paper. The measured Power Factor (PF) is adjusted to a required value using FGS based PID controller. If the measured PF is different from the required reference value an error signal is generated. This error signal and change of error are evaluated by FLC to obtain the new constants values for the PID controller that used to drive six-pulse full wave thyristorized rectifier circuit, which can thus control the excitation field voltage. A VAR compensation for the weak bus, with a desired PF, has been applied on the modified IEEE-5 bus sample systems using bifurcation analysis and Q-V sensitivity methods as voltage stability indicator. In this paper, a suitable model of the SM has been presented. Loading and no load conditions in addition to excitation field voltage have been tested. A good agreement between practical and theoretical results has been observed.

Simulation results demonstrate that better control performance can be achieved in comparison with Ziegler-Nichols controllers and Kitamori's PID controllers. It has been found that the proposed controller (FGS based PID) provides fast response, flexible, nonlinear gain characteristic and adaptive operation. It is concluded that the reactive power compensation system with a FGS based PID controller of SM is reliable, sensitive, economical, faster, and more efficient with no harmonics.

Keywords: Reactive Power Compensation, PID controller, Fuzzy Logic, Fuzzy Gain Scheduling, Voltage Stability, Bifurcation, and Matlab-Simulink.

تعويض القدرة الخيالية باستخدام جدولة الكسب المضبب للمسيطر التناسبي التكاملي المسيطر على الماكنة التزامنية

مأمون فاضل الكبابجي **أحمد نصر بهجت السماك**

قسم الهندسة الكهربائية - كلية الهندسة / جامعة الموصل

الخلاصة

يقدم هذا البحث نموذج لتطبيقات نظرية المنطق المضبب لجدولة الكسب للمسيطر التقليدي التناسبي التكاملي (PID) والذي بدوره يسيطر على تعويض القدرة الخيالية باستخدام الماكنة التزامنية. حيث تم في هذا البحث عرض نموذج مناسب للماكنة التزامنية مع أجراء فحوصات على هذا النموذج لحالات عديدة مثل التغير المفاجئ في الحمل أو في فولتية تغذية المجال فضلاً عن حالات الحمل واللاحمل. قورنت نتائج نموذج الماكنة التزامنية الذي تم بناؤه بواسطة برنامج محاكات المتلاب بالنتائج العملية وظهر تطابقاً جيداً بينهما. قورن أداء المسيطر التقليدي بي أي دي (PID) المصمم والمسيطر الذكي المصمم ذي جدولة الكسب المضبب (FGS) عند استخدامه للسيطرة على سوق دائرة تقويم سداسية النبضة لموجة كاملة التحكم والتي بدورها نظمت تغذية المجال للماكنة التزامنية، لإعطاء قدرة التعويض (KVAR) اللازمة للحصول على عامل القدرة المحدد. طبق هذا العمل على نظام (IEEE- 5bus) باستخدام تحليل التشعيب (Bifurcations) وتحسس تغير الفولتية مع القدرة الخيالية (VQ-Sensitivity) كمؤشر لاستقرارية الفولتية.

المسيطر PID المبني على FGS أبدى سرعة في الأداء مرونة وخاصية لا خطية للكسب مقارنة مع غيره من المسيطرات. أظهر المسيطر ذو جدولة الكسب المضبب (FGS) ان القدرة المعوضة هي أكثر وثوقية وأكثر حساسية واقتصادية وأكثر كفاءة وبأقل ما يمكن من التوافقيات.

Received 27 Sep. 2007 **Accepted 26 March 2008**

List of Symbols:

va,vb, vc and ia, ib and ic = Thee phase terminal voltages (V) and terminal current (A) respectively.

α= Firing angle (degree).

V_f and I_f= DC field voltage (V) and DC field current (A).
R_f, L_{ff} = Resistance of field circuit (ohm) and self of rotor inductance (henry) respectively.
L_a, L_b and L_c= Stator self inductance (static)/ phase (henry).
L_{ab}, L_{bc} and L_{ca}= Mutual inductance between stator Phases (henry).
L_{af}, L_{bf} and L_{cf}= mutual inductances between stator phases and rotor (henry).
L_s= Part of phase inductance harmonic because of salience (henry).
λ_a, λ_b and λ_c= Instantaneous linkage flux for stator phases (Wb).
[V], [R], [i], [λ] and [L]= Voltage, resistance, current, linkage flux and voltage matrix respectively.
T_e and T_m= Electrical and mechanical torques (N.m) respectively.
ω_s and ω_r = Synchronous and rotor speed (rpm).
θ= Displacement angle for rotor refers to stator phase (a) (rad).
P= Number of pair poles.
P_L&Q_L = Real and reactive power load demand respectively (watt, var).
P_m&Q_m = Real and reactive power of the synchronous motor respectively (watt, var).
P_t&Q_t = total real and reactive power for the synchronous motor and load demand respectively (watt, var).
K_p, K_I, K_d = Proportional, Integral, and derivative gain for the PID control respectively.
K_{cr}= critical value gain for the PID control which give sustained oscillations output of system.

1. Introduction:

Electric power system equipment and other industry inductive loads draw reactive power. The increasing demand of reactive power does really have its own major impact on the generating units, lines, circuit breakers, transformers, relays and isolators. More reactive power demand results in increasing dimensions and cost which reduce the whole power system efficiency.The required reactive power can be compensated from any other source [2-4].

In this paper, controlled reactive power compensation is investigated in a single Synchronous Machine (SM) connected to infinite bus system with load. This SM was used to control the reactive power compensation. A suitable model of the SM has been presented. Loading and no load conditions in addition to excitation field voltage have been tested. A good agreement between practical and theoretical results has been observed. The details SM tests are given in IEEE Standards documents [5, 6].

The best-known controllers used in industrial control processes are proportional-integral-derivative (PID) controllers because of their simple structure and robust performance in a wide range of operating conditions. The PID controllers in the literature can be divided into two main categories. In the first category, the controller parameters are fixed during control after they have been tuned or chosen in a certain optimal way [7]. The controllers of the second category have a structure similar to PID controllers, but their parameters are adapted on-line based on parameter estimation, which requires certain knowledge of the process, e,g., the structure of the plant model [8]. Such controllers are called adaptive PID controllers in order to differentiate them from those of the first category. The application of knowledge-based systems in process control is growing, especially in the field of fuzzy

control [9-16], in fuzzy control, linguistic descriptions of human expertise in controlling a process are represented as fuzzy rules or relations.

In this work, a rule-based scheme for Gain Scheduling (GS) of PID controllers is proposed for process control [11]. It is demonstrated that human expertise on PID GS can be represented in fuzzy rules. Furthermore, better control performance can be expected in the proposed method than that of the PID controllers with fixed parameters, where FL is not considered as a logic, but as a computing method. Fuzzy systems are considered from two points of view. First, the system has linguistic representation with linguistic variables and fuzzy if-then rules. Second, FL is used as a numerical method to create a nonlinear mapping between inputs and outputs.

2. Synchronous Machines (SM):

Direct 3-phase model of SM is adopted in this paper, the machine parameters and variables are expressed in their actual physical quantities. This model is more suitable in studying all normal and abnormal conditions. Thus, it is easy to monitor directly the machine variables and parameters without transformation. The direct 3-phase model of the SM can be adopted with the following assumptions:

1. The machine is assumed magnetically linear.
2. The inductance variation is considered sinusoidal with the rotor position.
3. Eddy currents and hysteresis effects are neglected.

Based on these assumptions, the direct 3-phase model of the SM can thus be represented by the following equations (1-6) [17-19]:

$$[V]=[R]\cdot[i]+p\{[L]\cdot[i]\}, \text{ or } [V]=[R]\cdot[i]+p[\lambda] \quad \ldots(1)$$

where p represented the derivative pointer.

$$\left.\begin{array}{l}[i]=[i_a \quad i_b \quad i_c \quad i_f]^t,\ [R]=diag[R_a \quad R_b \quad R_c \quad R_f] \\ [V]=[v_a \quad v_b \quad v_c \quad V_f]' \text{ and } p[\lambda]=[p\lambda_a \quad p\lambda_b \quad p\lambda_c \quad p\lambda_f]'\end{array}\right\} \quad \ldots(2)$$

Since, the relationship between leakage flux and current is:

$$[\lambda]=[L]\cdot[i] \quad \ldots(3)$$

Differentiating two sides of equation (3) gives:

$$p[\lambda]=[L]\cdot p[i]+\frac{d[L]}{d\theta}\cdot[i]\cdot p\theta \quad \ldots(4)$$

where matrixes [L] and $\frac{d[L]}{d\theta}$ are given in Ref.[18]. Rearranging equation (4) would result in:

$$p[i]=[L]^{-1}\left\{[V]-[R]\cdot[i]'-\frac{d[L]}{d\theta}\cdot[i]p\theta\right\} \quad \ldots(5)$$

The total electrical developed torque would thus be [17]:

$$T_e=0.5\cdot p\cdot[i]\cdot\frac{d[L]}{d\theta}\cdot[i] \text{ and } T_e=T_m+K\cdot\omega_r+KD\frac{d\delta}{dt}+J\frac{d\omega}{dt} \quad \ldots(6)$$

All equations from (1) to (6) were modeled and simulated using Matlab7.2 -Simulink.

SM is characterized by its ability either to produce or to absorb reactive power, Q. When this machine operates at unity PF, it will neither produce nor absorb reactive power (Q = 0). SM has its operating limits, determined by its capability curve that should not be exceeded in order to keep them at rated operational conditions. Figure (1-a) shows typical motor capability curves [4].

A motor can be operated safely in the thick encircled area of Figure (1-a). The stator current limit is the maximum continuous current that the stator conductors can carry without being damaged. The rotor current limit is the maximum field current or excitation current that the DC excitation system can carry. These rated currents are usually found in the machine nameplate.

The intensity of the field current is related to the machine's PF, and hence, the production or absorption of Q. Figure (1-b) shows a plot of the armature current I_A versus field current I_f which is called the V-curve.

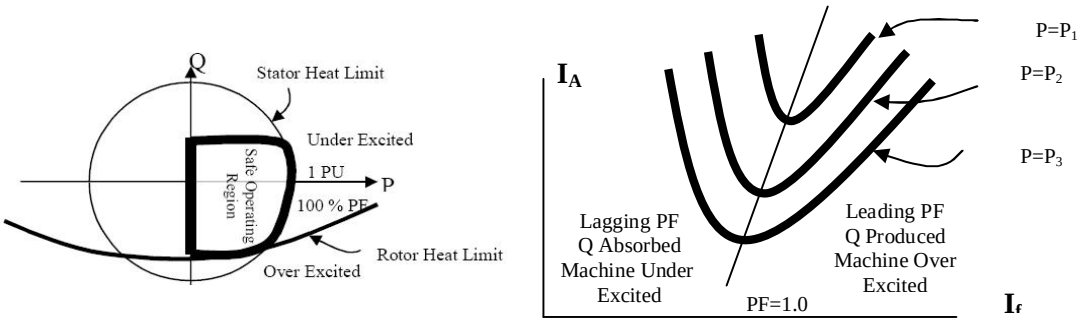

(a) (b)

Figure (1) Synchronous Motor Capability Curves and V-Curves [4].

2.1 Excitation Field Voltage: The excitation field voltage, which controls the reactive power of the machine [18, 19], was modeled using six-pulse rectifier circuit where the basic equations were derived as follows; the output DC voltage Vf1 equal to:

$$Vf1 = \frac{n}{2\cdot\pi}\cdot\int_{\frac{\pi}{2}-\frac{\pi}{n}+\alpha}^{\frac{\pi}{2}+\frac{\pi}{n}+\alpha} Vp\cdot\sin(\omega t)\cdot d(\omega t) \text{ or, } Vf1 = \frac{n\cdot\sqrt{3}}{2\cdot\pi}\cdot Vp\cdot\cos(\alpha) \quad \ldots(7)$$

Where n &Vp represent numbers of phases and peak voltage respectively.

After adding free-wheeling diode on the DC output circuit, equation (7) will become: $(\text{for } (\alpha)\geq 60^o)$

$$Vf_2 = \frac{n}{2\cdot\pi}\cdot\int_{\frac{\pi}{2}-\frac{\pi}{n}+\alpha}^{\frac{5\pi}{6}} Vp\cdot\sin(\omega t)\cdot d(\omega t) \text{ or, } Vf_2 = \frac{n\cdot\sqrt{3}}{4\cdot\pi}\cdot Vp\cdot(1+\cos(\alpha)-\frac{1}{\sqrt{3}}\cdot\sin(\alpha)) \quad \ldots(8)$$

As a result from the above analysis, the relationship between firing angle (α) and DC output voltage of the six pulse rectifier circuit with free- wheeling diode shown in Figure (2) where the DC field voltage (V_f) depending on the thyristor trigger angle (α) would be as follows:

$$Vf = Vf_1 \quad \text{for } 0\leq(\alpha)\leq 60^o, \text{and } Vf = Vf_2 \quad \text{for } (\alpha)\geq 60^o \qquad \ldots(9)$$

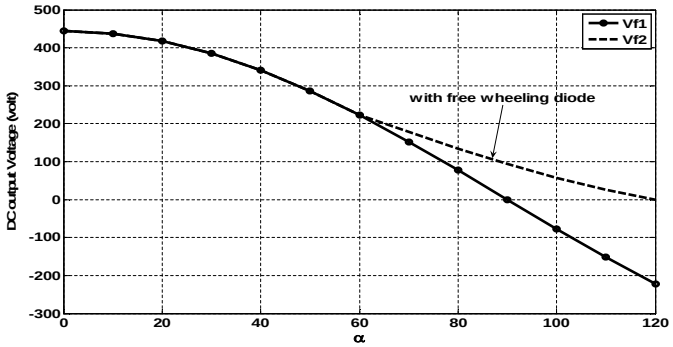

Figure (2) The relationship between DC field voltage (Vf) and firing angle (α).

3. Load Flow Study:

Load flow calculations provide power flows and voltages for a specified power system subjected to the regulating capability of generators, condensers, and OLTC transformers as well as specified grid interchange between individual operating systems [20, 21]. Newton Raphson method is applied to analyze, in steady state, the modified IEEE 5-bus test systems as given in Appendix (B). Results give the solution to determine reactive power demand in order to maintain system voltage stability.

4. Modal Analysis for Voltage Stability Evaluation:

Several algorithms have been developed to study voltage stability and to detect how the system is close to voltage collapse. All of these algorithms assess the distance between the present loading and the bifurcation set in the space of load demands, which are also used to determine weak area/bus. In this study, only the V-Q sensitivity method is adopted, which is considered as powerful methods [21].

4.1 V-Q Sensitivity Method: In any power system, if at any system bus the voltage magnitude increases as its injected reactive power is increased the system voltage would be stable. On the contrary, the system voltage would be unstable if, for at least one bus in the system, its voltage magnitude decreases as the injected reactive power at that bus is increased. In other words, a system voltage is stable if V-Q sensitivity is positive for every bus and unstable if V-Q sensitivity is negative for at least one bus [22].

So in any system, buses can be arranged from their weakest bus to the strongest one using the V-Q sensitivity method as given in the following sub-sections where weak buses are those that show the higher participation factors to the smallest eigenvalues. In this work, this V-Q sensitivity method which is adopted to determine the system weak bus at which the SM is to be connected for VAR/PF control, has been applied to modified IEEE 5-bus sample systems [22].

4.1.1 Reduced Jacobian Matrix: The linearized steady state system power voltage equations are given by [22],

$$\begin{bmatrix} \Delta P \\ \Delta Q \end{bmatrix} = \begin{bmatrix} J_{P\theta} & J_{PV} \\ J_{Q\theta} & J_{QV} \end{bmatrix} \cdot \begin{bmatrix} \Delta \theta \\ \Delta V \end{bmatrix} \quad \ldots(10)$$

where: $\Delta P, \Delta Q$ = incremental change in bus real and reactive power respectively.
and $\Delta V, \Delta \theta$ = incremental change in bus voltage magnitude and angle respectively.

If the conventional power-flow model is used for voltage stability analysis, the Jacobian matrix in (10) is the same as the Jacobian matrix used when the power-flow equations are solved using the Newton-Raphson technique.

System voltage stability is affected by both P and Q. However, at each operating point keeping P constant and evaluate voltage stability by considering the incremental relationship between Q and V. This is analogous to the Q-V curve approach. Although incremental changes in P are neglected in the formulation, the effects of changes in system load or power transfer levels are taken into account by studying the incremental relationship between Q and V at different operating conditions.

Substituting $\Delta P = 0$ at equation (10) to reduce this equation and thus resulting in the following:

$$\left.\begin{aligned} \Delta Q &= \left[J_{QV} - J_{Q\theta} \cdot J_{P\theta}^{-1} \cdot J_{PV} \right] \cdot \Delta V \text{ or, } \Delta Q = J_R \cdot \Delta V \text{ and, } \Delta V = J_R^{-1} \cdot \Delta Q \\ \text{where, } J_R &= \left[J_{QV} - J_{Q\theta} \cdot J_{P\theta}^{-1} \cdot J_{PV} \right] \end{aligned}\right\} \quad \ldots(11)$$

where J_R is called the reduced Jacobian matrix of the system. J_R is the matrix, which directly relates to the bus voltage magnitude and bus reactive power injection. Eliminating the real power and angle part from the system steady state equations are allowed to focus on the study of the reactive demand and supply problem of the system as well as minimizing computational effort [23].

5. Conventional Control System (PID):

One widely used controller in industrial process control is the PID (three-term) controller. This controller whose transfer function is generally written in the "parallel form" or as the "ideal form" is given by equation (12):

$$G(s)=K_P+K_I\cdot\frac{1}{s}+K_D\cdot s \quad \text{or;} \quad G(s)=K_P\cdot\left(1+\frac{1}{T_I\cdot s}+T_D\cdot s\right) \qquad \ldots(12)$$

This controller provides a proportional term, an integration term, and a derivative term [7]. The time domain output is given by equation (13):

$$u(t)=K_P\cdot e(t)+K_I\cdot\int e(t)\cdot dt+K_D\cdot\frac{de(t)}{dt} \qquad \ldots(13)$$

where K_P is the proportional gain, K_I the integral gain, K_D the derivative gain, T_I the integral time constant and T_D the derivative time constant.The individual effects of these three terms on the closed-loop performance are summarized in Table (1).

Table (1) Effects of Independent P, I, and D Tuning.

Closed-Loop Response	Rise Time	Overshoot	Settling Time	Steady-State Error	Stability
Increasing K_P	Decrease	Increase	Small Increase	Decrease	Degrade
Increasing K_I	Small Decrease	Increase	Increase	Large Decrease	Degrade
Increasing K_D	Small Decrease	Decrease	Decrease	Minor Change	Improve

5.1 Tuning Objectives and Existing Methods: PID controller parameters are tuned such that the closed-loop control system would be stable and meet given objectives associated with the following:

- Stability robustness and Set-point following and tracking performance at transient, including rise-time, overshoot, and settling time.
- Regulation performance at steady-state, including load disturbance rejection;
- Noise attenuation and robustness against environmental uncertainty.

In this work, PID Controller parameters were tuned to give high performance for the reactive power compensation by controlling the firing angle (alpha) of the six-pulse rectifier circuit. Ziegler and Nichols (ZN) rules [7, 8] were chosen with some tuning to determine values of the K_P, K_I, and K_D. In this method (ZN) first K_I and K_D are set to zero. Using the proportional control (K_P) action only, shown in Figure (3), to evaluate critical gain value Ku. By increasing (K_P) from 0 to specific value, as shown in Figure (4), the output first exhibits sustained oscillations at K_p=14. Then T_u is calculated from the experimental result shown in Figure (5). This method suggests setting the values of parameters K_P, K_I, and K_D each according to the formula shown in Table (2).

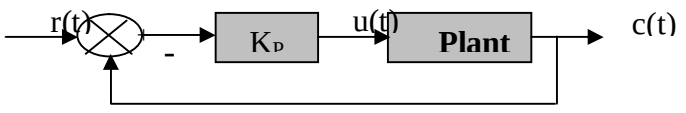

Figure (3) Closed – loop system with a proportional controller.

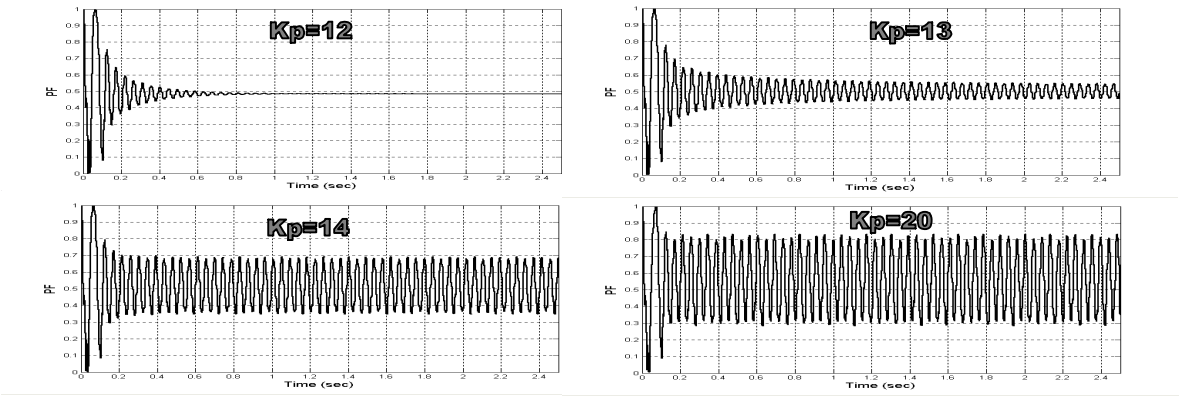

Figure (4) Power factor (PF) vs time, when PID controller was tuned by a change of proportional gain (K_P) from 12-20.

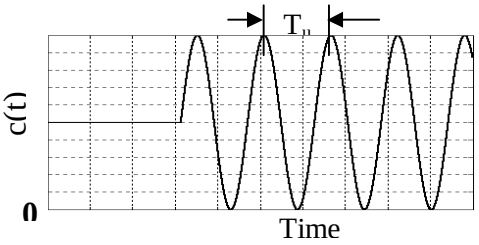

Figure (5) Sustained oscillation vs time.

Table (2) ZN tuning rules [24].

Type	K_P	$T_I = \frac{K_P}{K_I}$	$T_d = \frac{K_d}{K_P}$
P	**0.5Ku**	**0**	**0**
PI	**0.45Ku**	**T_u/1.2**	**0**
PID	**0.6Ku**	**T_u/2**	**T_u/8**

6. Fuzzy Gain Scheduling (FGS):

Gain scheduling means a technique where controller parameters (gains) are changed during control in a predefined way. It is not always counted as an adaptive control [10], but it enlarges the operation area of a linear controller to perform well also with a nonlinear system, defines it as follows:

Gain Scheduling (GS): a linear parameter varying feedback regulator whose parameters are changed as a function of operating conditions [10].

The system schedules the controller parameters according to predefined parameter values with respect to changing operation conditions. Scheduling variables can be the measured signal, the controller output signal or an external signal, i.e., whatever signal tells the current state of operation conditions. By using intelligent technical, a fuzzy supervisor can be adopted for GS. It is used only to store the tuning parameters and respective operation conditions in memory and to compute correct values of the parameters for current conditions as done later. FL offers smooth transition between operation conditions, a flexible and natural way to code the parameter values and the operation points to a rule base. The fuzzy supervisor schedules the parameters of the conventional controller according to the nonlinearities of the process. Input to the fuzzy block can be any signal indicating a change in operation conditions which demands different values for the control parameters. Conventional GS involves using extra information from the plant, environment, or users to tune (via "schedules") the gains of a controller. The overall scheme is shown in Figure (6).

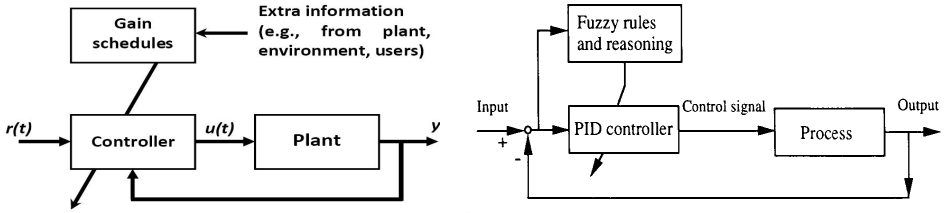

(a) **(b)**

Figure (6) Conventional and intelligent GS, where
(a) Conventional GS [10]. (b) PID control system with a FGS [11].

It is to be noted that Figure (6-a) could be viewed as a GS approach in control field, which would come up with a fixed mapping between operating conditions, plant data, and external inputs (e.g., the user inputs) and the controller parameters. The fuzzy system is a static nonlinear just like many conventional gain schedules, and it simply offers another type of interpolator for GS. Figure (6-b) shows the PID control system with a FGS.

It is assumed that Kp and Kd are in prescribed ranges [Kpmin, Kpmax] and [Kdmin, Kdmax], respectively. The appropriate ranges are determined experimentally. For convenience, Kp and Kd are normalized into the range between zero and one by the following linear transformation:

$$Kp' = \frac{(Kp - Kp_{\min})}{(Kp_{\max} - Kp_{\min})} \text{ and, } \quad Kd' = \frac{(Kd - Kd_{\min})}{(Kd_{\max} - Kd_{\min})} \qquad \ldots(14)$$

In the proposed scheme, PID parameters are determined based on the current error e(k) and Δe(k), . The integral time constant is determined with reference to the derivative time constant, i.e.,

$$Ti = \alpha.Td \qquad \ldots(15)$$

and the integral gain is thus obtained by: $Ki = \frac{Kp}{\alpha.Td} = \frac{Kp^2}{\alpha.Kd}$ …(16)

The parameters $Kp', Kd' \text{ and } \alpha$ are determined by a set of fuzzy rules as:

if e(k) is Ai and $\Delta e(k)$ *is Bi then* Kp' *is Ci,* Kd' *is Di, and* $\alpha = \alpha_i$

i=1,2,3,…..,m. …(17)

Here, Ai, Bi, Ci, and Di are fuzzy sets of the corresponding sets; α_i is a constant. The membership function (MF) of these fuzzy sets, are as shown in Figure (7) and (8). In these Figure, PB represents positive big, PM positive medium, and so on. Fuzzy sets Ci and Di may be either Big or Small and are characterized by the membership functions shown in Figure (7) and given in the following equation (18):

$$x_{small}(\mu) = e^{-4\cdot\mu} \text{ and, } x_{Big}(\mu) = 1 - e^{-4\cdot\mu} \qquad \ldots(18)$$

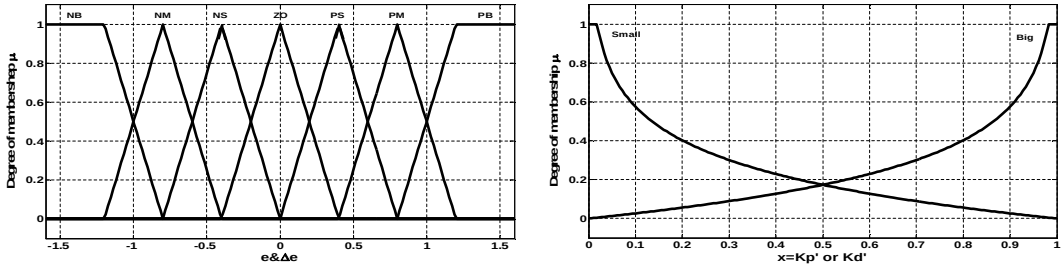

(a) **(b)**

Figure (7) Membership function for: (a) e(k) and $\Delta e(k)$ **(b) Kp' and Kd'**

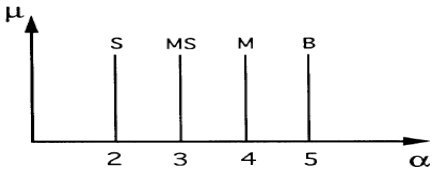

Figure (8) Singleton membership functions for α .

Fuzzy rules in equation (24) may be extracted from operator's expertise. Here the rules experimentally based on the step response of the process would be derived. Figure (9) shows an example of a desired time response.

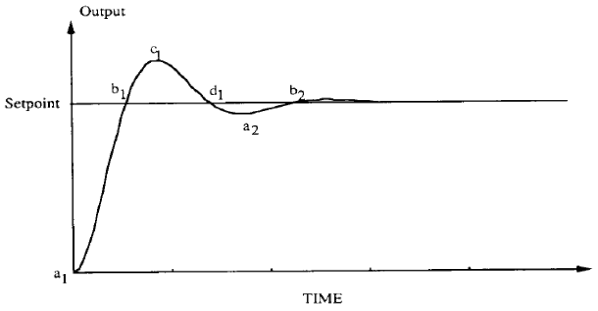

Figure (9) Process step response.

At the beginning, i.e., around a1, a big control signal would be required in order to achieve a fast rise time. To produce a big control signal, the PID controller should have a large proportional gain, a large integral gain, and a small derivative gain. Thus the proportional gain (Kp') can be represented by a fuzzy set Big, and the derivative gain (Kd') by a fuzzy set Small. The integral action is determined with reference to the derivative action as in equation (15). For the PID controller, taking a small α or a small integral time constant Ti will result in a strong integral action. Whether the integral action should be strong or weak is determined in the scheme by comparison with the well-known Ziegler-Nichols (ZN) PID tuning rule. In the ZN rule, the integral time constant Ti is always taken four times as large as the derivative time constant [11]. That is, α is equal to 4. In the proposed scheme, α takes a value less than 4 (say 2) to generate a "stronger" integral action. Therefore, the rule around a1 reads:

if e(k) is PB and $\Delta e(k)$ is ZO then Kp' is Big, Kd' is Small, and $\alpha = 2$

Note that α may also be considered as a fuzzy number which has a singleton membership function as shown in Figure (10). For example α becomes 2 when α is small.

A round point b1 in Figure (9), a small control signal would be expected in order to avoid a large overshoot. That is, the PID controller should have a small proportional gain, a large derivative gain, and a small integral gain. Thus the following fuzzy rule is taken:

if e(k) is ZO and $\Delta e(k)$ *is NB then* Kp' *is Small,* Kd' *is Big, and* $\alpha = 5$

Thus a set of rules shown as tables in Appendix (C), such that B stands for Big, and S for Small.

The truth-value of the ith rule in equation (17) μ_i is obtained by the product of the MF values in the antecedent part of the rule [11], as given in equation (19):

$$\mu_i = \mu_{Ai}[e(k)] \cdot \mu_{Bi}[\Delta e(k)] \qquad \ldots(19)$$

where μ_{Ai} is the MF value of the Fuzzy set Ai given a value of e(k), and μ_{Bi} is the MF value of the Fuzzy set Bi given a value of $\Delta e(k)$.

Then, the defuzzification yields the following equation (20):

$$Kp' = \sum_{i=1}^{m} \mu_i \cdot Kp'_i, \; Kd' = \sum_{i=1}^{m} \mu_i \cdot Kd'_i \text{ and } \alpha = \sum_{i=1}^{m} \mu_i \cdot \alpha_i \qquad \ldots(20)$$

Here Kp'_i is the value of Kp' corresponding to the grade μ_i for the ith rule, as shown in Figure (10). Kd'_i is obtained in the same way. Once Kp', Kd' and α are obtained, the PID controller parameters are calculated from equations (14-20), where Kpmin, Kpmax, Kdmin, and Kdmax are given in Appendix (C).

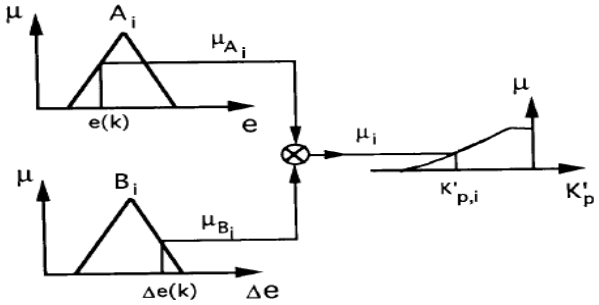

Figure (10) Implication process of a fuzzy rule [11].

7. SM Modeling and Simulation:

The overall system model for reactive power compensation at week bus system is shown in Figure (11), where SM is modeled and simulated on Matlab7.2-Simulink. All equations of this model are given in detail in Section (2). Ref [19] gives the SM rating and parameters. The practical and calculated results for the change in speed and phase current (i_a) of synchronous motor driving mechanical load varying from 5N.m to zero (no load) are shown in Figure (12), where these results prove the simulation method validity [13].

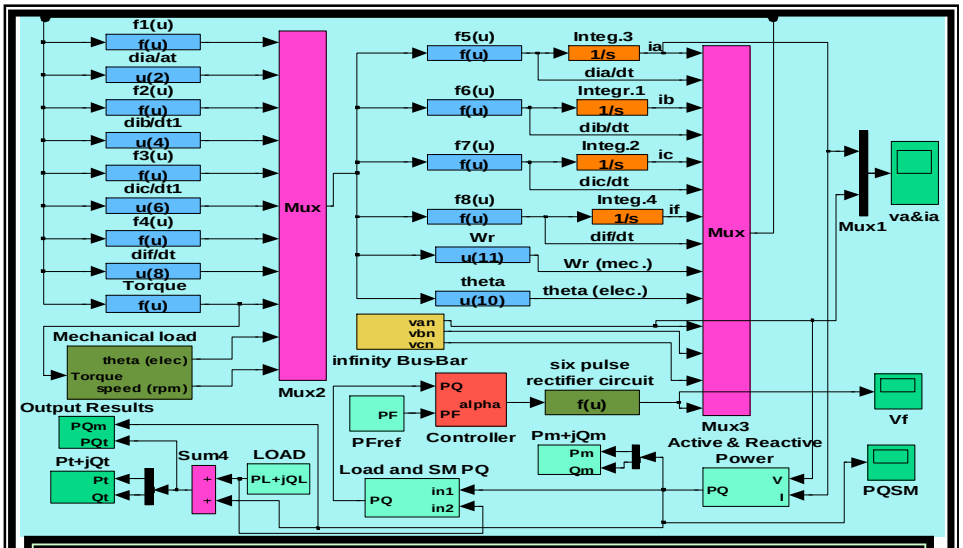

Figure (11) The overall main system model (weak bus with SM compensation and load) modeled in Matlab-Simulink [13].

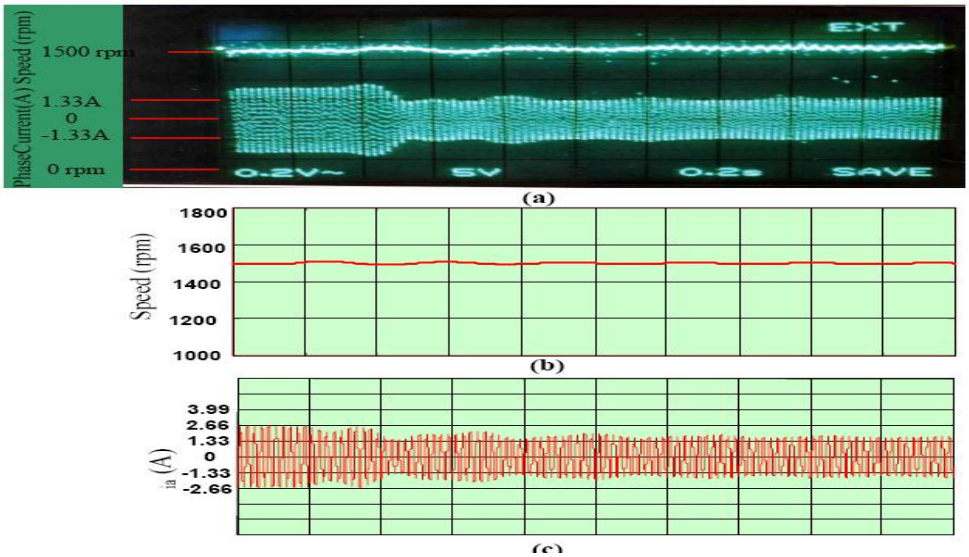

Figure (12) Speed and phase current for synchronous motor connected to infinity bus-bar when the load changes from 5N.m to zero(no load), where: (a) Practical result. (b)&(c) computer results. Note: time axis equal to *200msec/division,*

8. Excitation control circuit of SM for reactive power control:

The conventional control (PID), gives good results for PF or VAR control, but the parameters of PID controller must be changed when the SM state is to be changed from lagging to leading PF conditions [13]. Figure (13) shows the off-line tuning double PID controllers where the switch here is used for selection the truth controller which in turn gives the dip in results due to inverse output of lagging PF controller, this problem can be solved by limiting and anti-windup controller output [13]. These PID controllers are shown in Figure (11) with SM. Figures (14-18) show the performances of SM and its PID controller with constant load (both P_L and Q_L). The results show oscillations before reaching steady state error and thus leading to some harmonics and distortions in excitation field voltage as shown in Figure (15-a). Instantaneous voltage and current are illustrated in Figures (17, 18).

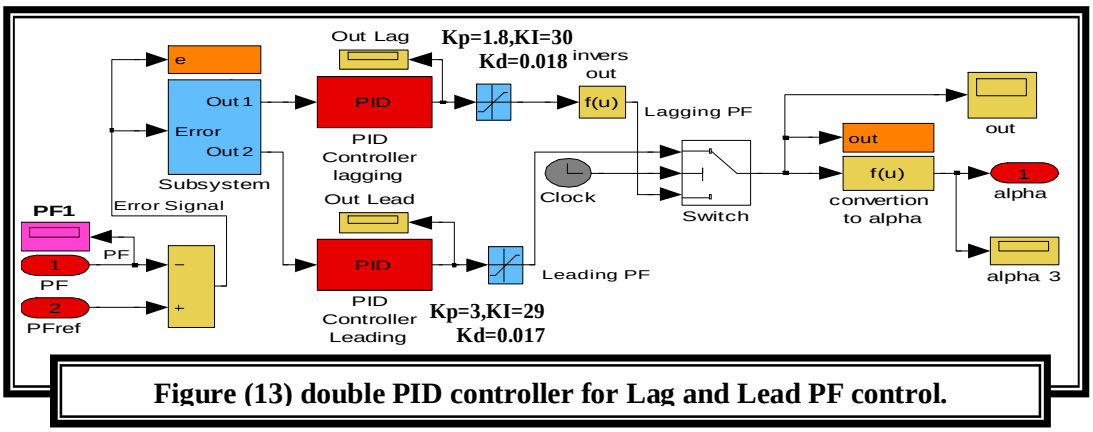

Figure (13) double PID controller for Lag and Lead PF control.

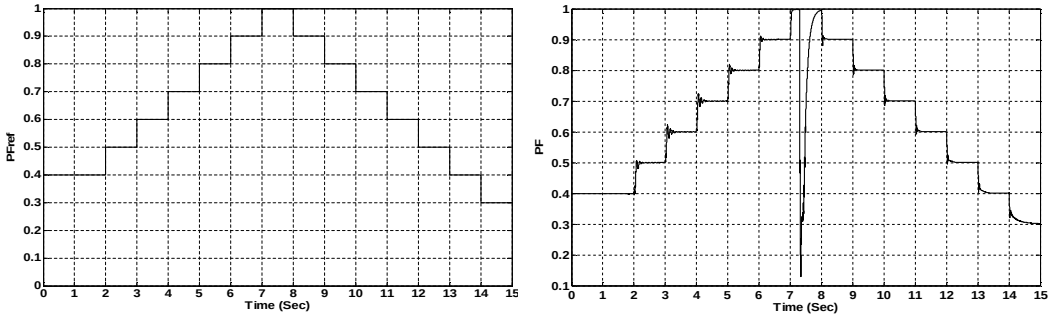

(a) **(b)**

Figure (14) PF variation vs time of double PID Controllers.

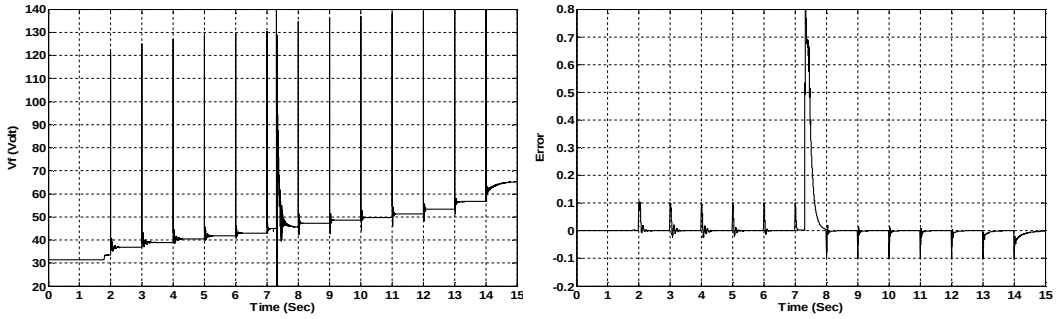

(a) **(b)**

Figure (15) Field voltage and error signal vs time of double PID Controllers.

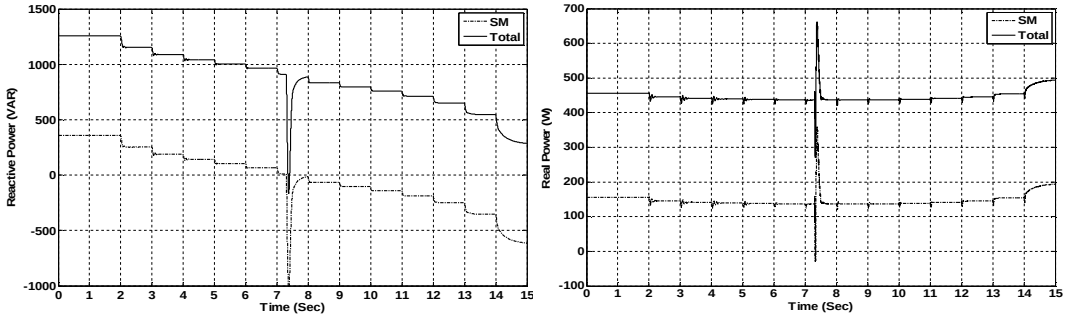

(a) **(b)**

Figure (16) Q and P variation vs time of double PID Controllers.

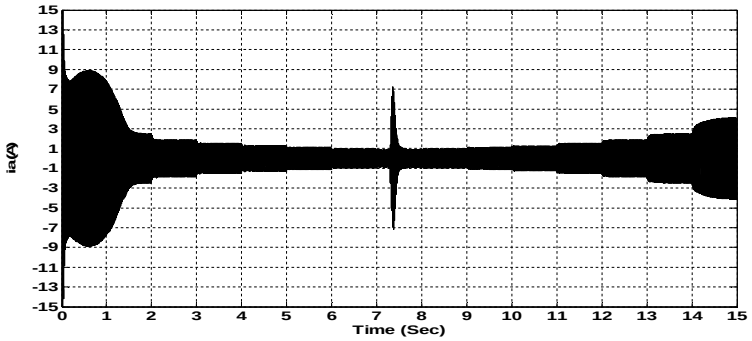

Figure (17) SM instantaneous phase current (i_a) variation vs time of double PID Controllers.

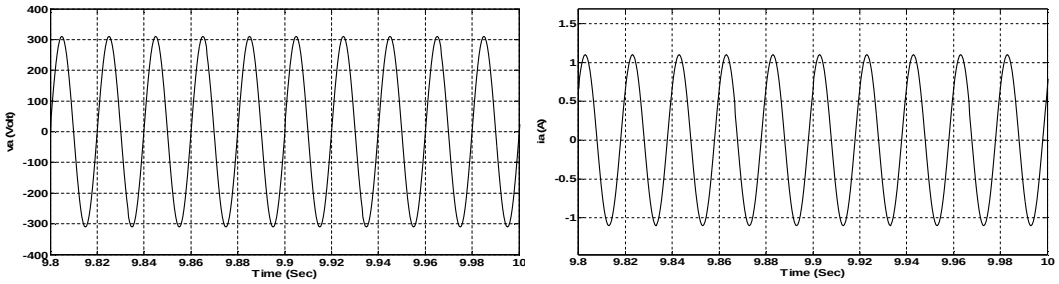

(a) **(b)**

Figure (18) Focused SM instantaneous voltage and current variation vs time of double PID Controllers: (a) Terminal voltage (va). (b) Phase current (ia).

In this work, intelligent control system used to control PF/VAR of SM can be FGS based PID Controller, using Mamdani's method. The FGS scheme has been tested on a variety of processes as designed in detail in Section (6). The FGS based PID controller as modeled in Matlab-Simulink is shown in Figure (19) [13].

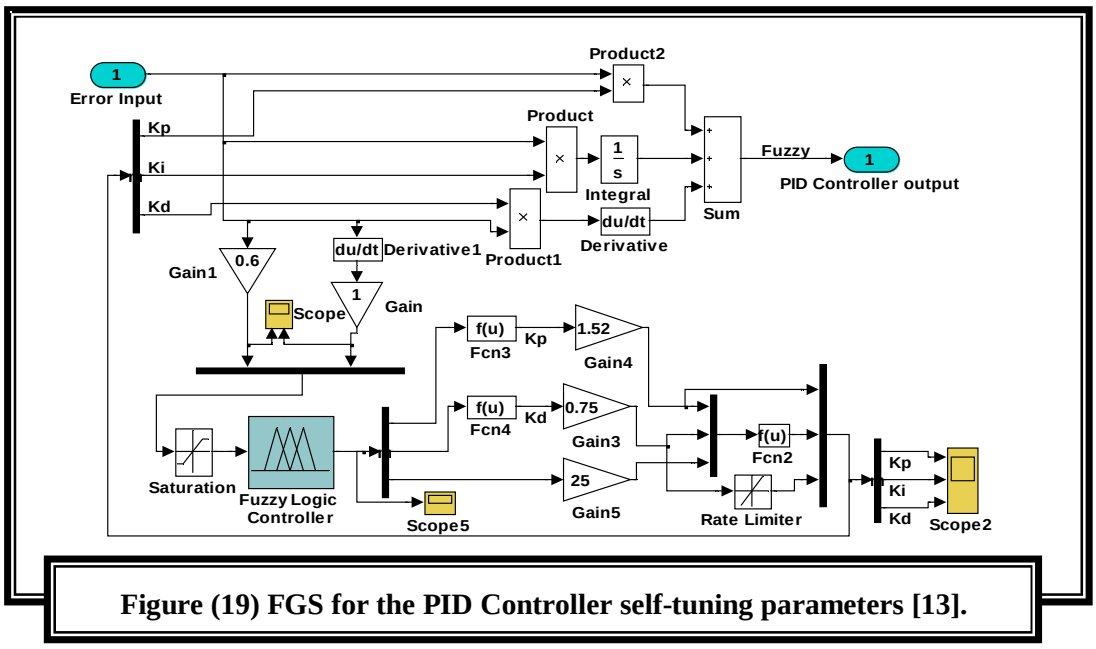

Figure (19) FGS for the PID Controller self-tuning parameters [13].

FGS has two fuzzy variables error (e) and change of error (Δe) and seven linguistic variables for each, from negative big to positive big, as shown in Figure (20). The FGS attributes and all details are given in following summary:

name: 'ahmedfuzzy'**; type:** 'mamdani'; **andMethod:** 'min'**; orMethod:** 'max'.
defuzzMethod: 'centroid'; **impMethod:** 'min'.; **aggMethod:** 'max'.
input: [1x2 struct]; **InLabels** = e, De ; **output:** [1x3 struct]; **outLabels** = Kpr, Kdr, alphar.
rule: [1x49 struct].

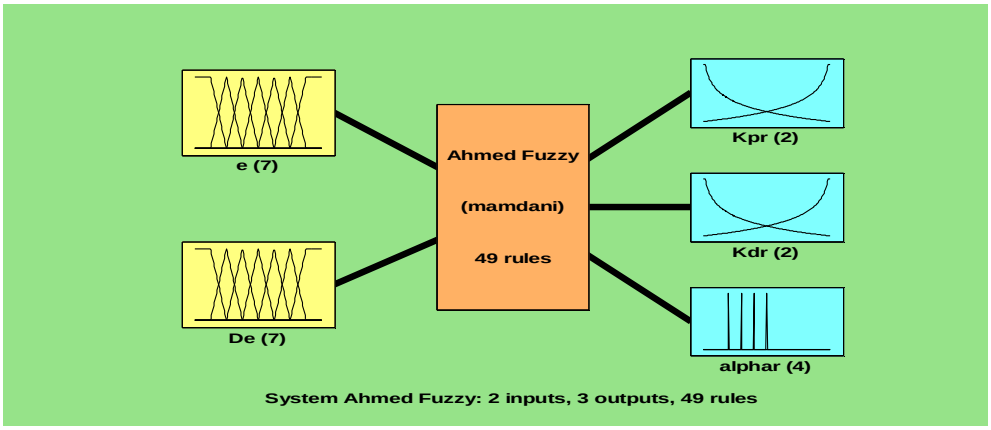

Figure (20) Fuzzy Logic overall diagram [13].

Time responses of tested second, third and fourth order functions, given in equations (21-23) [11], are shown in Figure (21).

$$G1(s) = \frac{e^{-0.5 \cdot S}}{(s+1)^2} \quad \ldots(21)$$

$$G2(s) = \frac{4.228}{(s+0.5) \cdot (s^2 + 1.64s + 8.456)} \quad \ldots(22)$$

$$G3(s) = \frac{27}{(s+1) \cdot (s+3)^3} \quad \ldots(23)$$

The results obtained by using ZN-PID controllers and Kitamori's PID controllers are also presented for comparison, with FGS, as shown in Figure (21). Figure (22) shows the PID parameters determined by the FGS for controlling 4th order process while the two inputs to FGS are shown in Figure (23). The Fuzzy control surface (three-dimension plotter mapping between inputs and output) is shown in (24).

The above simulation shows that a variety of processes can be satisfactorily controlled by the FGS based PID controller. This control method is used to control the excitation field voltage of SM to give the required reactive power. Runge-Kutta 4th order solver is implemented in the Matlab-Simulink7.2 package to process the simulation results. Figure (25) shows the SM PF performance results using FGS based PID controller depending on steps of PFref shown in Figure (14-a).

The results of the proposed FGS of double PID controller are shown in the Figures (25-29). As compared to the conventional double PID controller, the on-line FGS self and auto tuning double PID controller can thus be able to completely overcome leading PF overshoot with an approximately 70% reduction of settling time, while it can approximately reduce the lagging PF overshoot by 40% and settling time by 50%. It is important to note that such a great enhancement is obtained by utilizing this FGS method disregarding any change in the SM operating characteristic. The proposed controller completely meets the design specifications mentioned in Section (6). The results obtained by using conventional PID controllers and FGS based PID controllers are also presented for comparison, as shown in Figure (29). Table (3) shows the comparing maximum swiftness parameters results between conventional PID, and FGS based PID controllers [13].

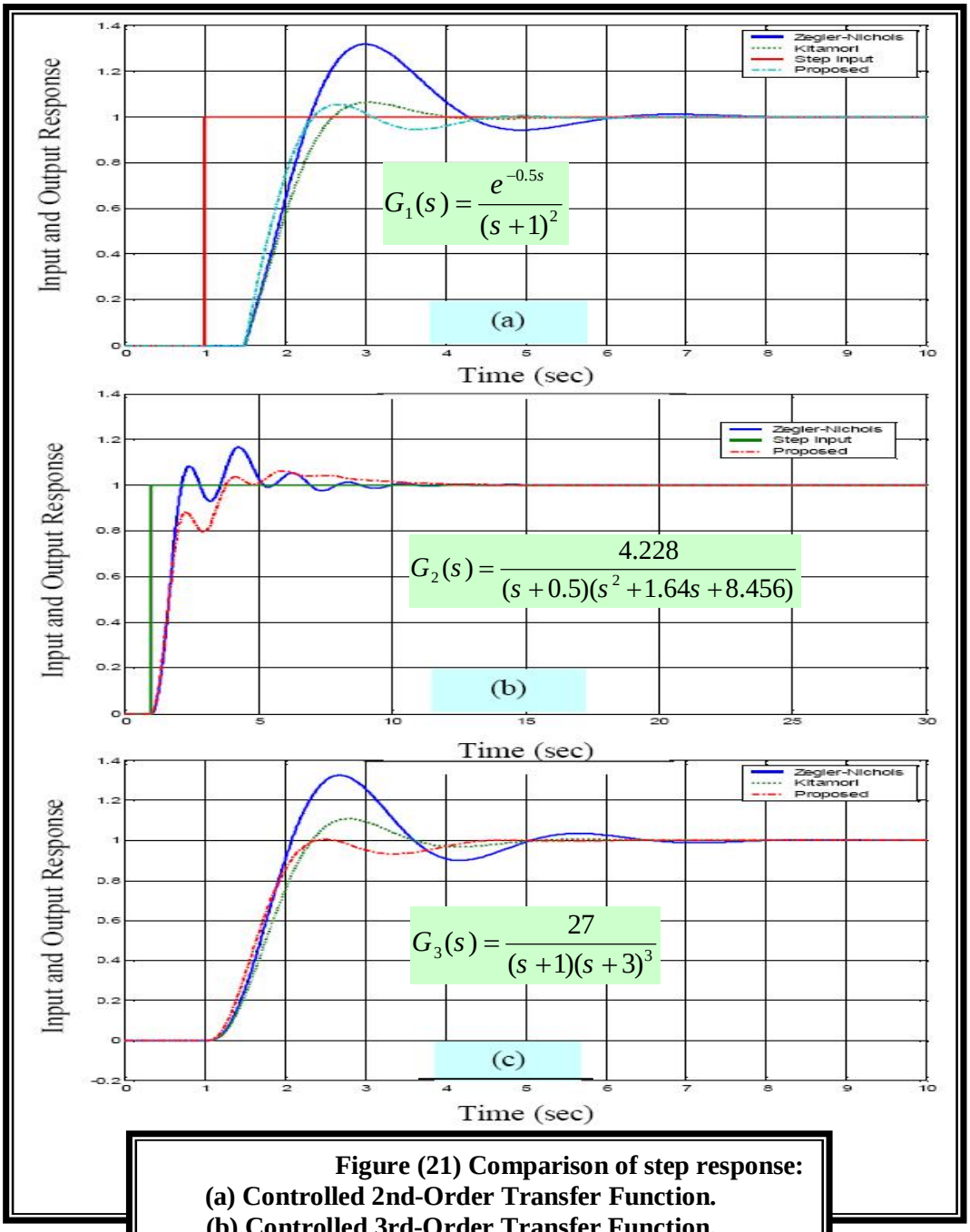

Figure (21) Comparison of step response:
(a) Controlled 2nd-Order Transfer Function.
(b) Controlled 3rd-Order Transfer Function.
(c) Controlled 4th-Order Transfer Function.

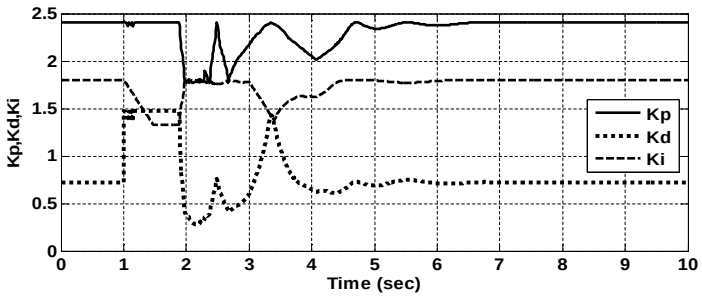

Figure (22) PID parameters of the FGS controller to control 4th order process.

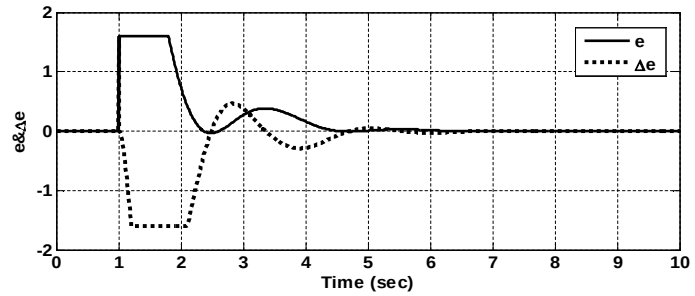

Figure (23) Error and change of error for 4th order process equation (23).

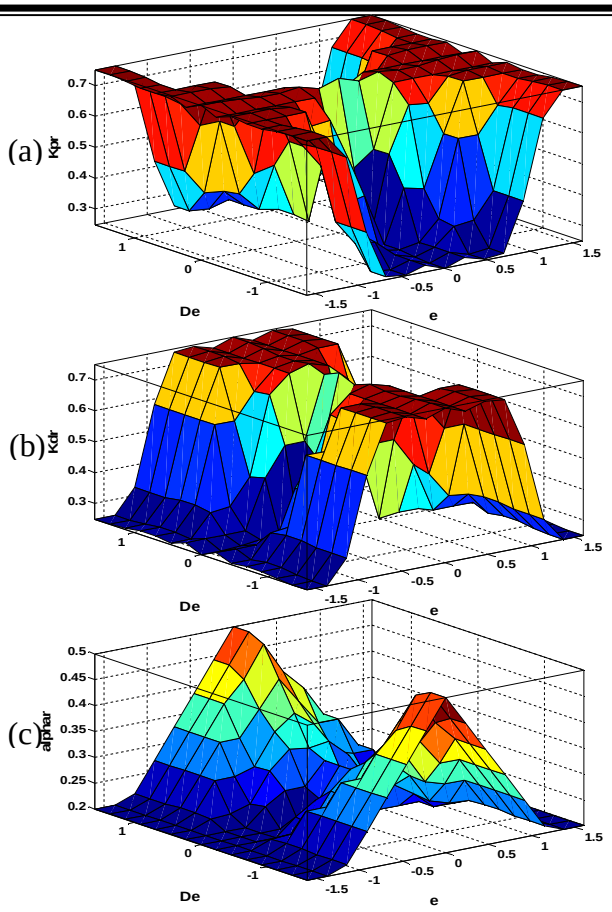

Figure (24) Fuzzy control surface 3-output Kpr, Kdr, and alphar respectively, which gives Kp, Kd, and Ki as given in section (6).

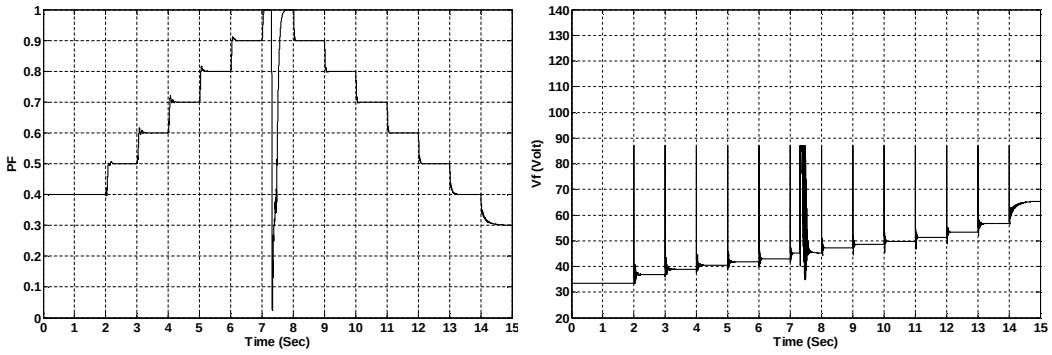

(a) **(b)**

Figure (25): (a) SM power factor (PF) variation vs time using FGS.
(b) Excitation field voltage (Vf) variation vs time using FGS.

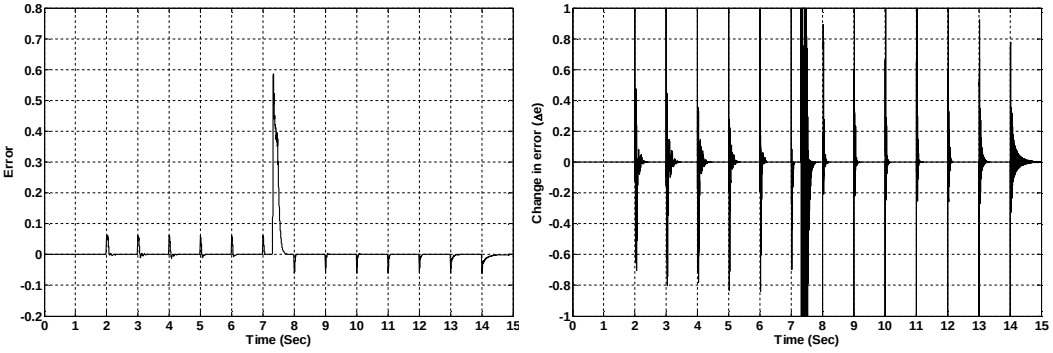

(a) **(b)**

Figure (26) Error and change in error signals variation vs time using FGS.

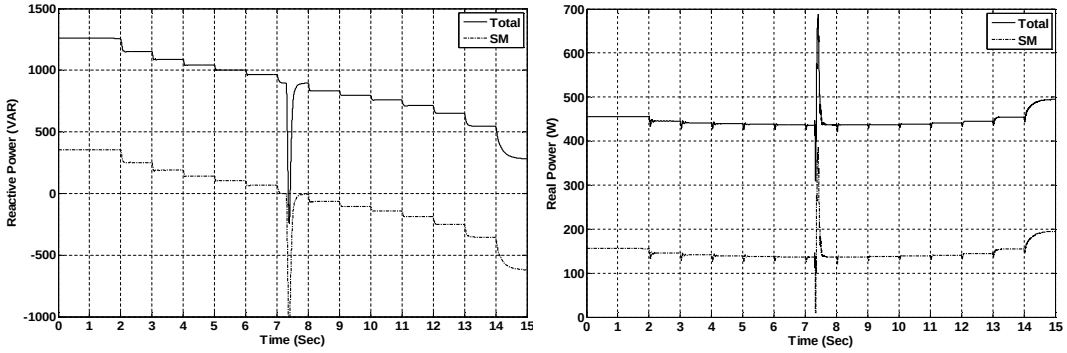

(a) **(b)**

Figure (27) Reactive power and real power variation vs time using FGS.

Table (3) Response of maximum swiftness parameters vs types of control.

Control Method	Rise Time (T_r) %		Peak Time (T_P) %		Settling Time (T_s) %		Perc. Overshoot (P.O.)%	
	Lag	Lead	Lag	Lead	Lag	Lead	Lag	Lead
Conventional PID	4.1	2	5.8	2	38	25	3.5	-2
FGS Based PID	2.7	2.11	6.3	5.8	25	6	2.5	-0.4

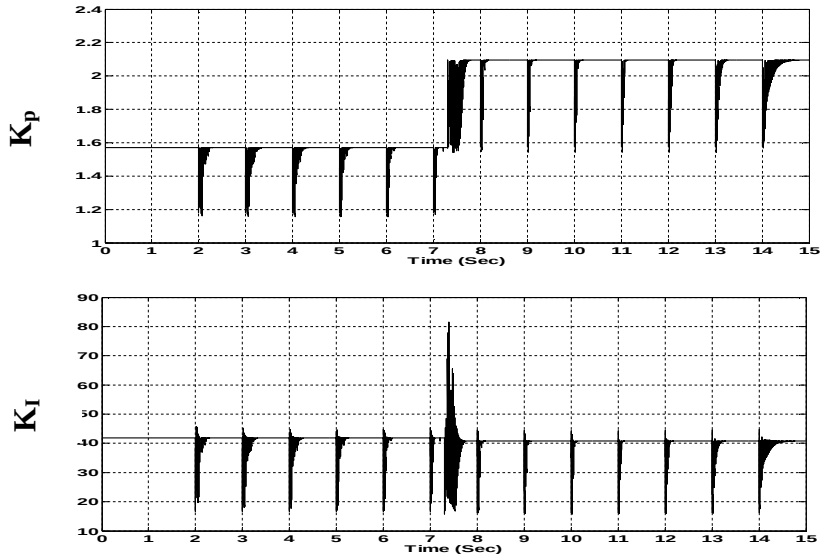

Figure (28) PID parameters of the FGS based PID controller of SM.

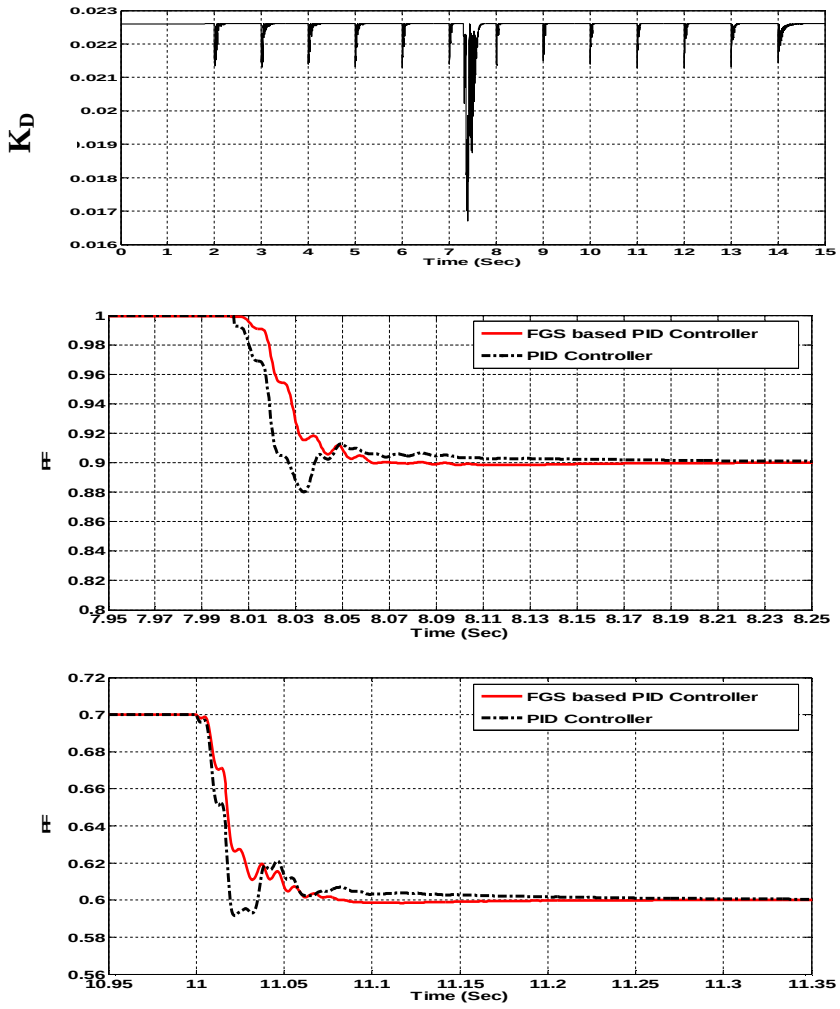

Figure (29) SM power factor (PF) variation vs time comparing between conventional PID controllers and FGS based PID controllers.

9. Load Flow and Voltage Stability Assessment:

Load flow results for the modified IEEE 5-bus with SM compensation are given in Appendix (B).Voltage stability can be assessed using several methods, as given in Section (4). In this work, the results adopted on bifurcation analysis and Q-V sensitivity methods. Figure (30) shows a Modified IEEE 5-Bus sample system as modeled in Matlab7.4-Simulink, Power System Analysis Toolbox (PSAT).

Direct Methods (DM) for computing Saddle-Node Bifurcation (SNB) points and Limit-Induced Bifurcation (LIB) points have been used. The bifurcation analysis result for modified IEEE 5-bus system shown in Figures (31).

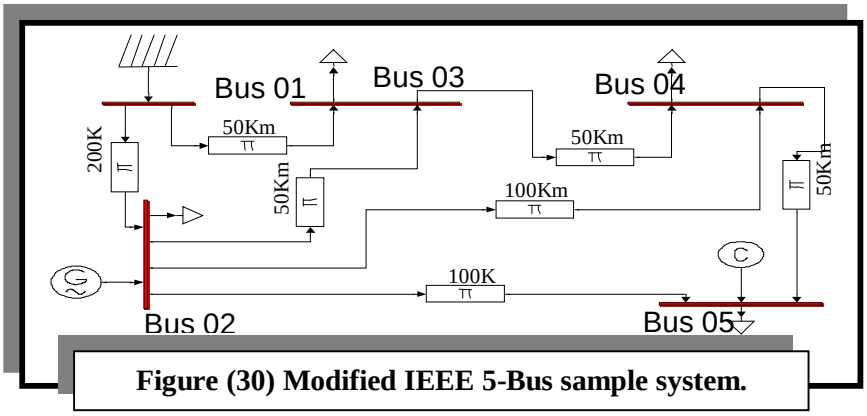

Figure (30) Modified IEEE 5-Bus sample system.

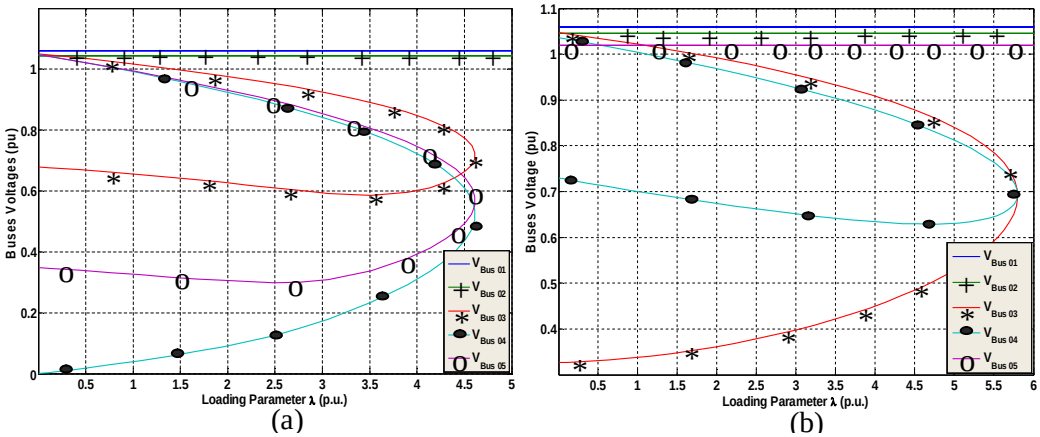

(a) (b)

Figure (31): Nose curves for the modified IEEE 5-bus test system with generator reactive power limits. The maximum loading condition is due to a saddle limit-induced bifurcation, where:

(a) Without SM compensator. (b) With SM compensator at bus 5.

In any system, buses can be arranged from their weakest bus to the strongest bus (infinity bus) using the V-Q sensitivity method. Weak buses are those buses which show higher participation factors to the smallest eigenvalues. In this work, this V-Q sensitivity method has been applied to the modified IEEE 5-bus sample system; all detailed analyses are given in Appendix (D). Table (4) show the effect of compensation at bus-5 on the system weak buses configuration for the modified IEEE 5-bus. These results can thus show that bus-5 has been changed from weakest bus state to a strong bus state resulting in improving the overall system voltage stability.

Table (4) Bus weakness sequence from weakest to less weak bus:

(a) Without compensation at bus-5.

(a)

Weakness order	1.	2.	3.
Bus No.	5	4	3

(b) With compensation at bus-5.

(b)

Weakness order	1.	2.
Bus No.	4	3

10. Conclusions:

Controlled reactive power compensation is investigated in a single machine connected to infinite bus system with load. A controller introduced depends on the dynamic behavior of SM analysis. This machine is used to control the total reactive power absorbed by the load. Conventional (PID) and intelligent controllers (FGS based PID controller) have been designed, implemented and compared to output control signal used to drive six-pulse full wave thyristorized rectifier circuit which can thus control the excitation field voltage. The SM (working as motor) will produce the needed kVAR, for the desired PF to the weak bus. **All the conclusions arrived would be divided into the following categories:**

- PID controller has been designed and implemented in such a way to give high performance due to good off-line tuning of PID parameters.
- PID controllers are often not properly tuned (e.g., due to plant parameter variations or operating condition changes), there is a significant need to develop methods for the continuous tuning PID controllers gains. A FGS has been designed and implemented to on-line changing the PID controller parameters which adjust the PID gains to obtain improved performance actions.
- FGS gives better performances and results as compared to conventional PID controller owing to its continuous smooth coverage of the whole PF range from its zero-Lag to zero-Lead limits. The results show that a smooth variation with step input changes due to very small maximum instantaneous PF error in both lagging and leading PF as compared with other controllers (such as PID). It also shows that maximum instantaneous PF error equal to 4% in leading PF and equal to 6% in lagging PF with steady state error equal to zero.
- The designed FGS based PID performance overcome output response overshoot in both of the over or under compensations. The main benefits of this designed FGS system would thus exist in more flexibility, fast (about three cycles), more efficient, reliable and economical.
- Synchronous motor can be used as a dynamic reactive power compensator for constant loads and a voltage regulator for variable loads, which would in turn increase the system voltage stability owing to converting this weak load bus into strong bus by overcoming the reactive load demand.
- Bifurcation analysis and Q-V sensitivity methods have been used to calculate system weak buses which are characterized by showing higher participation factors to the smallest Eigen-values. These methods have been applied on modified IEEE 5-Bus sample system using Matlab7.4-Simulink, PSAT. The weak load bus has been chosen for the SM reactive power compensation that would hence in turn result in improving the overall system voltage stability.

References:

[1] **Çolak, R. Bayindir,** "A Novel Dynamic Reactive Power Compensator Based on PIC", Electric Power Components and Systems, Taylor & Francis Inc., No.33, **2005**, Pages 861–876.

[2] **Richard C. Schaefer,** "Excitation Control of the Synchronous Motor", IEEE Transactions on Industry Applications, Vol. 35, No. 3, May/June 1999, Pages 694-702.

[3] **W. Xu, J. R. Marti, and H. W. Dommel,** "Harmonic Analysis of System with Static Compensator", IEEE Transactions on Power Systems, Vol. 6, No.1, Feb. **1991**, Pages 183-190.

[4] **M. M. Al-Hamrani, A. Von Jouanne, and A. Wallace,** "Power factor correction in industrial facilities using adaptive excitation control of synchronous machines", IEEE Pulp and Paper Industry Technical Conference, 17-21 June **2002** Pages 148 – 154.

[5] **IEEE Std**, "IEEE Guide: Test Procedures for Synchronous Machines", Rotating Machinery Committee of the IEEE Power Engineering Society, 115-**1983**.

[6] **IEEE Std**, "IEEE Standard for High-Potential Test Requirements for Excitation Systems for Synchronous Machines", Energy Development and Power Generation Committee of the IEEE Power Engineering Society, 421.3-**1997**.

[7] **K. Ogata**, "Modern Control Engineering", Second Edition, Prentice-Hall, Inc. **1995**.

[8] **J.G. Ziegler, and N.B. Nichols**, "Optimum settings for automatic controllers", Transactions of ASME, Vol 64, Nov. **1942**, pp.759-768.

[9] **L. A. Zadeh**, "Fuzzy sets," Information Control, vol. 8. pp. 338-353, **1965**.

[10] **K.M. Passino and S. Yurkovich**, "Fuzzy Control", Addison Wesley Longman, Inc., **1998**.

[11] **Z.-Y. Zhao, M. Tomizuka, and S. Isaka**, "Fuzzy gain-scheduling of PID controllers," IEEE Trans. Syst., Man,. Cybern., Vol. 23, **1993**, pp.1392–1398.

[12] **G. Kilic, and I.H. Altas**, "Power Factor Correction of Synchronous Motor Using FL", Mathematical & Computational Applications, Vol.1, No.1, **1996**, pp. 66-72.

[13] **Ahmed. N. Al-Sammak,** "A Fuzzy Logic Control of Synchronous Motor for Reactive Power Compensation", Ph.D. thesis, Electrical Engineering Department, University of Mosul, **2007**.

[14] **P.Ya. Ekel and etal.**, "FL Technology in Reactive Power Control", IEEE International Conference on Electric Utility Deregulation and Restructuring and Power Technologies **2000**, City University, London, 4-7 April **2000**. pp.518-523.

[15] **Çolak, R. Bayindir, and I. Sefa,** "Experimental study on reactive power compensation using a FL controlled synchronous motor", Energy Conversion and Management, No. 45, **2004**, pp. 2371–2391.

[16] **A. D. Grey**, "Power Factor Improvement using FL Control of an AC Synchronous Motor", SoutheastCon, Proceedings IEEE 8-10 April, **2005**, pp. 193-199.

[17] **S. M. Al-Haj Zber,** "Modeling and Computer Simulation of a Current Source Inverter Fed Synchronous Motor Drive System", Msc thesis, Electrical Engineering Department, University of Mosul, **2000**.

[18] **M. F. Al-Kababji and Ahmed N. Al-Sammak,** "Modeling & Simulation of Synchronous Machine Controlled by PID Control for the Reactive Power Compensation", JIEEEC, Proceedings of the 6th Jordanian International Electrical & Electronics Engineering Conference, Jordan, Vol.2, **2005**, pp. 339-346..

[19] **M. F. Al-Kababji and Ahmed N. Al-Sammak,** "Adaptive Neuro-Fuzzy Inference System (ANFIS) Real Time Based Power Factor Control by Synchronous Machine", 1st EEC07, 26-28 June, **2007**, FEEE, University of Aleppo-Syria, PS-5, pp.1-24.

[20] Ahmed. N. Al-Sammak, "A New Method for Transient Stability Study, with Application to INRG", Msc thesis, Electrical Engineering Department, University of Mosul, **1999**.

[21] IEEE/PES Power System Stability Subcommittee Special Publication, "Voltage Stability Assessment, Procedures and Guides", Final Version, December **2000**.

[22] Federico Milano, Power System Analysis Toolbox (Matlab), Documentation for PSAT version 1.3.4, July 14, **2005.**

[23] Carson W. Taylor, "Power System Voltage Stability", McGraw-Hill Inc., **1994**.

APPENDIX (A): The Power Station and Transmission System Model Rating and Parameters:

Power=160MVA, f=50Hz, Voltage=220Kv, Current=422A, and Impedance=303Ω.

The transmission line (100Km TL) rating and Parameters are:

Voltage=220Kv, f=50Hz, R=7e-6□/Km, X=0.03e-3 □/Km, and C=60e-3 nF/Km.

APPENDIX (B): Theoretical Load Flow Result for the Modified IEEE 5-Bus Sample System with SM Compensator:

POWER FLOW REPORT

NETWORK STATISTICS

Bus:	5
Lines:	7
Generators:	2
Synchronous Compensator:	1
Loads:	4

SOLUTION STATISTICS

Number of Iterations:	3
Maximum P mismatch [p.u.]	0
Maximum Q mismatch [p.u.]	0
Power rate [MVA]	100

POWER FLOW RESULTS

Bus	V [p.u.]	phase [rad]	P gen [p.u.]	Q gen [p.u.]	P load [p.u.]	Q load [p.u.]
Bus 01	1.06	0	33.8959	8.0415	0	0
Bus 02	1.045	-0.09469	0.64	35.9692	12.8	12.8
Bus 03	1.0206	-0.06757	0	0	9.6	11.2
Bus 04	1.0007	-0.08959	0	0	6.4	16
Bus 05	1.0131	-0.10098	0	6.4	4.8	6.4

LINE FLOWS

From Bus	To Bus	Line	P Flow [p.u.]	Q Flow [p.u.]	P Loss [p.u.]	Q Loss [p.u.]
Bus 02	Bus 03	1	-7.0013	9.9827	0.09845	0.42193
Bus 03	Bus 04	2	8.3481	4.6901	0.06365	0.27279
Bus 04	Bus 05	3	2.6501	-4.6115	0.02043	0.08754
Bus 02	Bus 04	4	0.83667	7.2757	0.07103	0.30442
Bus 02	Bus 05	5	2.2081	4.8608	0.03775	0.16177
Bus 01	Bus 02	6	8.3847	-0.27354	0.18118	0.77644
Bus 01	Bus 03	7	25.5112	8.3151	0.46336	1.9858

LINE FLOWS

From Bus	To Bus	Line	P Flow [p.u.]	Q Flow [p.u.]	P Loss [p.u.]	Q Loss [p.u.]
Bus 03	Bus 02	1	7.0997	-9.5608	0.09845	0.42193
Bus 04	Bus 03	2	-8.2845	-4.4173	0.06365	0.27279
Bus 05	Bus 04	3	-2.6297	4.699	0.02043	0.08754
Bus 04	Bus 02	4	-0.76564	-6.9712	0.07103	0.30442
Bus 05	Bus 02	5	-2.1703	-4.699	0.03775	0.16177
Bus 02	Bus 01	6	-8.2035	1.05	0.18118	0.77644
Bus 03	Bus 01	7	-25.0479	-6.3293	0.46336	1.9858

TOTAL GENERATION

REAL POWER [p.u.]	34.5359
REACTIVE POWER [p.u.]	50.4107

TOTAL LOAD

REAL POWER [p.u.]	33.6
REACTIVE POWER [p.u.]	46.4

TOTAL LOSSES

REAL POWER [p.u.]	0.93585
REACTIVE POWER [p.u.]	4.0107

APPENDIX (C):

Based on an extensive simulation study on various processes, a rule of thumb for determining the range of Kp and the range of Kd is given as [34]: **Kp_{min}=0.32 K_u , Kp_{max}=0.6 K_u , Kd_{min}=0.08 $K_u.T_u$ and Kd_{max}=0.15 $K_u.T_u$,** where K_u and T_u are, respectively, the gain and the period of oscillation at the stability limit under P-control. The following tables represent fuzzy tuning rules for the FGS based PID method:

Fuzzy Tuning Rules For Kp'	**Change of error $\Delta e(t)$**						
	NB	**NM**	**NS**	**ZO**	**PS**	**PM**	**PB**

Error $e(t)$	**NB**	B	B	B	B	B	B	B
	NM	S	B	B	B	B	B	S
	NS	S	S	B	B	B	S	S
	ZO	S	S	S	B	S	S	S
	PS	S	S	B	B	B	S	S
	PM	S	B	B	B	B	B	S
	PB	B	B	B	B	B	B	B
Fuzzy Tuning Rules For Kd'		**Change of error** $\Delta e(t)$						
		NB	**NM**	**NS**	**ZO**	**PS**	**PM**	**PB**
Error $e(t)$	**NB**	S	S	S	S	S	S	S
	NM	B	B	S	S	S	B	B
	NS	B	B	B	S	B	B	B
	ZO	B	B	B	B	B	B	B
	PS	B	B	B	S	B	B	B
	PM	B	B	S	S	S	B	B
	PB	S	S	S	S	S	S	S
Fuzzy Tuning Rules For α'		**Change of error** $\Delta e(t)$						
		NB	**NM**	**NS**	**ZO**	**PS**	**PM**	**PB**
Error $e(t)$	**NB**	S	S	S	S	S	S	S
	NM	MS	MS	S	S	S	MS	MS
	NS	M	MS	MS	S	MS	MS	M
	ZO	B	M	MS	MS	MS	M	B
	PS	M	MS	MS	S	MS	MS	M
	PM	MS	MS	S	S	S	MS	MS
	PB	S	S	S	S	S	S	S

APPENDIX (D): V-Q Sensitivity Analysis Results of Modified IEEE-5 bus System

D.1 before compensation:

```
EIGENVALUE REPORT
P S A T  1.3.1
File:  E:\Program Files\MATLAB\R2006a\psat\ahmed\5-bus\d_sample05withoutSMC.mdl
Date:  14-Jun-2007 20:47:22

EIGENVALUES OF THE STANDARD POWER JACOBIAN MATRIX

Eigevalue      Real part                    Imaginary Part

Eig J1f1        1267.4693      0
Eig J1f2        226.6419       0
Eig J1f3        734.1478       0
Eig J1f4        999            0
Eig J1f5        999            0

PARTECIPATION FACTORS (Euclidean norm)
               Bus 01         Bus 02         Bus 03         Bus 04         Bus 05

Eig J1f1        0              0              0.50816        0.42295        0.06888
Eig J1f2        0              0              0.06624        0.34896        0.5848
Eig J1f3        0              0              0.4256         0.22809        0.34632
Eig J1f4        1              0              0              0              0
Eig J1f5        0              1              0              0              0

STATISTICS
NUMBER OF BUSES                5
# OF EIGS WITH Re(mu) < 0      0
# OF EIGS WITH Re(mu) > 0      5
# OF REAL EIGS                 5
# OF COMPLEX PAIRS             0
# OF ZERO EIGS                 0
```

D.2 after compensation at bus-5:

```
EIGENVALUE REPORT
P S A T  1.3.1
File:  E:\Program Files\MATLAB\R2006a\psat\ahmed\5-bus\d_sample05withSMC.mdl
Date:  14-Jun-2007 21:00:59

EIGENVALUES OF THE STANDARD POWER JACOBIAN MATRIX
Eigevalue      Real part                  Imaginary Part

Eig Jlf1        1223.8852      0
Eig Jlf2        544.5938       0
Eig Jlf3        999            0
Eig Jlf4        999            0
Eig Jlf5        999            0

PARTECIPATION FACTORS (Euclidean norm)
               Bus 01         Bus 02         Bus 03         Bus 04         Bus 05

Eig Jlf1        0              0              0.63454        0.36546        0
Eig Jlf2        0              0              0.36546        0.63454        0
Eig Jlf3        1              0              0              0              0
Eig Jlf4        0              1              0              0              0
Eig Jlf5        0              0              0              0              1

STATISTICS
NUMBER OF BUSES                5
# OF EIGS WITH Re(mu) < 0      0
# OF EIGS WITH Re(mu) > 0      5
# OF REAL EIGS                 5
# OF COMPLEX PAIRS             0
# OF ZERO EIGS                 0
```

The work was carried out at the college of Engg. University of Mosul